Volume 9, Issue 4, 2019, 4015 - 4021 **ISSN 2069-5837**

Biointerface Research in Applied Chemistry

www.BiointerfaceResearch.com

https://doi.org/10.33263/BRIAC94.015021

Original Research Article **Open Access Journal**

Received: 17.06.2019 / Revised: 03.08.2019 / Accepted: 10.08.2019 / Published on-line: 15.08.2019

Molecular docking and multitudinous spectroscopic studies to elucidating proton-pump inhibitor a lansoprazole binding interaction with bovine serum albumin

Manjushree Makegowda[1], Revanasiddappa Hosakere Doddarevanna[1,*], Chethan Kumar Mukundaswamy[2]

[1]Department of Chemistry, University of Mysore, Manasagangothri, Mysuru 570 006, Karnataka, India
[2]Postgraduate Department of Biochemistry, JSS College of Arts, Commerce and Science, Ooty Road, Mysuru 570 025, Karnataka, India
*corresponding author e-mail address:***hdrevanasiddappa@yahoo.com***

ABSTRACT

A carrier protein called bovine serum albumin (BSA) interaction with proton-pump inhibitor such as lansoprazole (LSE) has been investigated at 295, 303 and 311 K in pH 7.40 by docking and [UV–vis, CD, FT–IR and fluorescence (emission, 3D and synchronous)] spectroscopic studies. Emission fluorescence has suggested LSE−BSA complex formation by static quenching with strong binding. This interaction has proceeded by Vander Waals and hydrogen bonding. An observation from competitive site marker and docking experiments has resulted in binding of LSE with BSA transpired at site II, whereas from Förster's theory a binding distance (r) was retrieved to be 0.19 Å from LSE to Trp of BSA. Change in conformation, secondary structure and microenvironment of BSA were noticed after LSE interaction. Diminished binding constant in Zn^{2+}, Na^{+}, Fe^{2+}, Ca^{2+} and Co^{2+} ions presence on LSE-BSA interaction was also identified.

Keywords:*Bovine serum albumin, Binding studies, various fluorescence spectroscopy, Lansoprazole, Molecular docking.*

1. INTRODUCTION

Typical drug properties (metabolism, distribution, excretion and absorption) are significantly impacted by protein-drug binding. Wide assortments of organisms in the system of circulatory, serum albumins are exceedingly abundant proteins furnishes to osmotic blood pressure as being major macromolecule are also established in bodily secretions and tissues anywhere in the body; total albumin was comprised of extra-vascular protein about 60%. The current work is chosen BSA (Fig. 1A) as protein demonstrates due to its therapeutic significance, ready availability, unordinary ligand-binding properties and minimal cost [1, 2].

Lansoprazole (LSE) is medication to reduce long-lasting and pronounced acid from stomach production. LSE (Fig. 1B) is also used to treat indigestion, heartburn, persistent cough and difficulty in swallowing. LSE can block the enzyme at stomach wall that produces acid. The decreased acid production by enzyme blocking was allowed esophagus and stomach to heal. The fundamental side effects encircle blood disorders (leukopenia, pancytopenia, leukocytosis and thrombocytopenia), skin reactions (toxic epidermal necrolysis, erythroderma Stevens-Johnson syndrome and bullous eruption), myalgia, arthralgia, liver dysfunction, taste disturbance and peripheral oedema [3-5].

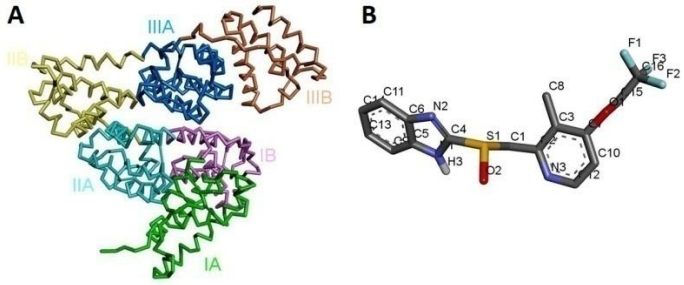

Figure 1.BSA (A) and LSE (B) three dimensional structures.

Functional and structural relationships of LSE under physiological circumstances can interact with BSA by molecular docking and numerous spectroscopic approaches were initiated to comprehend in this work. Effects of Zn^{2+}, Na^{+}, Fe^{2+}, Ca^{2+} and Co^{2+} ions on LSE−BSA interaction were inspected. Molecular basis and characterized chemical association resulted from these interaction investigations.

2. MATERIALS AND METHODS

2.1. Chemicals and stock solutions. LSE (≥98%, TLC), BSA (≥98%, chromatographically purified), digitoxin (≥92%, HPLC), ibuprofen (≥98%, GC), warfarin (98%, analytical standard), zinc chloride (≥99.999%, trace metal basis), sodium chloride (≥99%, ACS reagent), iron(II) sulphateheptahydrate (≥99%, ACS reagent), calcium chloride (≥93.0%, trace metal basis) and cobalt chloride hexahydrate (≥98%, ACS reagent) were procured from Sigma-Aldrich. The analytical standard was exploited for other chemicals. A stock solution of 1.0×10^{-3}mol L^{-1} was made for site markers, LSE and metal ions whereas 1.0×10^{-4}mol L^{-1} for BSA. All over experiments, Tris buffer (pH 7.40) prepared from double-distilled water was employed with proper background corrections.

2.2. UV-Vis measurements. DU 730 UV − visible Spectrophotometer (Life Sciences, Beckman Coulter, USA) was employed to BSA (3.30×10^{-6}mol L^{-1}) and LSE−BSA system to record absorption spectra at 303 K in 200–320 nm wavelength region. The concentration of LSE was varied from 0.0, 0.55, 1.10 up to 5.50 ($\times 10^{-6}$mol L^{-1}).

2.3. Circular dichroism spectral determinations. CD spectrum was come off on a Jasco circular dichroism spectropolarimeter (815, Japan) at 303 K for BSA (3.30×10^{-6}mol L^{-1}) and

LSE−BSA system. CD measurements were collected in 200–240 nm wavelength range and with scan speed 20 nm/min and bandwidth 1 nm. The concentration of LSE used was 66.0 $\times 10^{-6}$mol L^{-1}. BeStSel software online server was utilized for analysis of the secondary structure.

2.4. FT-IR spectroscopy. FT−IR spectrometer (Perkin Elmer, USA) attached with ATR accessory at 60 scans in 1700 to 1500 cm^{-1} range (303 K) was used to record spectra for BSA (subtracted with buffer) and LSE − BSA system (minus from buffer + LSE) with 4 cm^{-1} resolution. Concentration of LSE to BSA ratio is 30:1 at 3.30 $\times 10^{-6}$mol L^{-1}. ORIGINPRO 9.0 software was utilized for secondary structure evaluations by curve fitting assessments.

2.5. Fluorescence emission measurements. All fluorescence analysis was examined on Hitachi fluorescence spectrophotometer (F-4600, Japan) with 10 nm slit width using 150W Xenon lamp. Subtract an inner filter effect from each fluorescence spectrum for reducing its effect.

Fluorescence emission was noted down for BSA (3.30 $\times 10^{-6}$mol L^{-1}) with increased LSE (0.0, 0.55, 1.10 up to 5.50 $\times 10^{-6}$mol L^{-1}) concentrations at wavelengths of excitation at 295 nm and emission range from 295 to 430 nm at 295, 303 and 311 K. The needful temperature was acquired by utilizing external water shower.

2.6. Energy transfer between LSE and BSA. Spectra for BSA (3.30 $\times 10^{-6}$mol L^{-1}) and LSE (3.30 $\times 10^{-6}$mol L^{-1}) were recorded in fluorescence emission and UV−visible absorption, respectively at 303 K in 295−400 nm wavelength scan. These two spectra were overlapped to evaluate energy transfer parameters.

2.7. Synchronous fluorescence studies. Wavelength (excitation/emission) difference $\Delta\lambda$ (nm) at 15 for Tyr and 60 for Trp at 303 K was set to obtain LSE−BSA system's synchronous fluorescence spectra. The LSE concentrations varied (0.0, 1.10 up to 5.50 $\times 10^{-6}$mol L^{-1}) and BSA was maintained at 3.30 $\times 10^{-6}$mol L^{-1} in 210−320 nm scanning wavelengths.

2.8. 3D fluorescence studies. A ratio of 1:60 (3.30 $\times 10^{-6}$mol L^{-1}) for BSA to LSE at 303 K was made employed while noting downing 3D spectra in excitation (200−380 nm) and emission (250−500 nm) wavelengths.

2.9. Displacement experiments. Bearing site markers (3.30 $\times 10^{-6}$mol L^{-1}) with BSA (3.30 $\times 10^{-6}$mol L^{-1}) by increasing LSE (0.00 to 5.50 $\times 10^{-6}$mol L^{-1}), fluorescence emission spectra draw up at 303 K with monitored wavelengths (300−400 nm).

2.10. Metal ions on LSE − BSA binding. By varying LSE concentration (0.0 to 5.50 $\times 10^{-6}$mol L^{-1}), recorded the BSA (3.30 $\times 10^{-6}$mol L^{-1}) fluorescence spectra in metal ions (3.30 $\times 10^{-6}$mol L^{-1}) at 303 K ($\lambda_{ex} = 295$ nm) when λ_{em} = 290−420 nm.

2.11. Molecular docking. Structural geometry optimization of LSE (PMID: 3883) and BSA (PDB: 3V03) were refined on Marvin View and GROMOS96 force field. Docking and visualization were performed on AutoDockTools and 2016 Studio Discovery, respectively. The input was prepared for LSE and BSA to perform docking at three binding sites individually using grids 60 in all axes. Lamarckian genetic algorithm was exerted to cluster analysis at 100 runs.

2.12. Statistical assessments and explication of results. Mean ± standard deviation (SD) was adapted to each measurement as it done for 3 times. Microsoft Excel and OriginPro 9.0 employed as the tools for an explication of outcome results.

3. RESULTS

3.1. UV–Vis spectroscopy. BSA with various LSE concentrations shows the absorption spectrum (Fig. 2A) with decreased intensities of two peaks at 208 nm resulted from $\pi \rightarrow \pi^*$ transition (polypeptide backbone) and at 279 nm involved in the polarity of Trp/Tyr microenvironment [6, 7]. The redshift at 214 nm (~5 nm) was also encountered. These results have manifested that BSA conformational and polarity near Trp/Tyr microenvironment altered upon LSE interaction by forming complex as LSE−BSA.

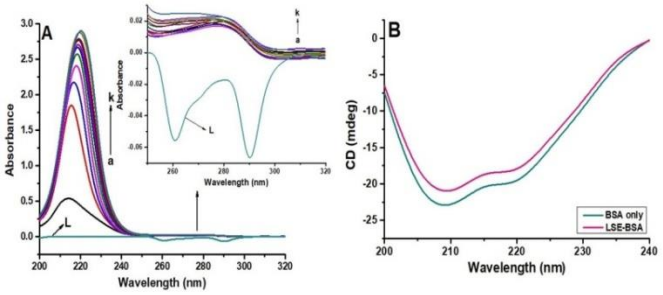

Figure 2. (A) UV−visible spectrum of LSE−BSA system with curve L is for LSE alone and (B) CD spectrum to BSA alone and LSE−BSA system at 303 K.

3.2. CD spectroscopy. Obtained CD spectrum with and without LSE for BSA (Fig. 2B) exemplifying negative bands one at 208 ($\pi \rightarrow \pi^*$) and anotherone at 220 nm ($n \rightarrow \pi^*$) characteristics to peptide bond α-helix content [8]. The reduced band intensities of BSA after LSE interaction is indicated that the secondary structure changes (Table 1).

3.3. FT − IR Measurements. Different vibrations in FT − IR spectra for proteins of numerous amide groups which exemplifying to peptide moiety. The absolute most broadly utilized is amide I for secondary structure evaluations. BSA alone and LSE−BSA system to FT−IR spectra at amide bands (I at 1700−1600 cm^{-1} for C = O and II at 1600−1500 cm^{-1} for N − H along with C − N) [9] exhibited in Fig. 3 and Table 2 to their spectral shifts. This demonstrates that LSE interacted with both C = O and C − N groups in polypeptides of BSA which supervises to carbonyl hydrogen bonding network rearrangement. Curve-fitted spectra at amide I to BSA and LSE−BSA system for the calculations of secondary structures by different components are represented in Fig. 4 and Table 1. Upon LSE interaction with BSA; α-helix, β-sheet and β-turns contents decreased whereas β-antiparallel and random coil are increased. Thus, this describes that BSA has undergone partial unfolding by changing its secondary structures with LSE.

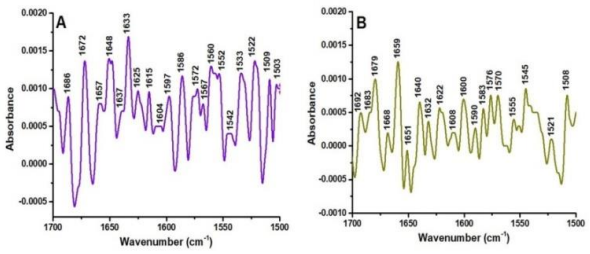

Figure 3.At 303 K, FT−IR spectra to BSA only (A) and LSE−BSA system (B).

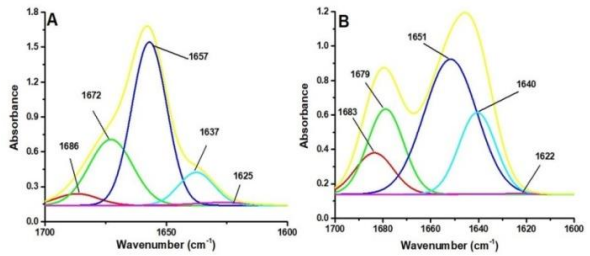

Figure 4. Amide I band undergone curve fitting by employing Gaussian peak function for (A) BSA alone and (B) LSE−BSA system.

3.4. Fluorescence Quenching. Considered intrinsic fluorescence for BSA caused by tyrosine (Tyr), phenylalanine (Phe), and Tryptophan (Trp) amino acids present in it. Trp alone is solely responsible for intrinsic fluorescence where it may alter when interacts with small molecules, which is common responding to subunit association, substrate binding and conformational transition. BSA fluorescence emission intensity (Fig. 5) decreases after LSE addition at maxima 343 nm (λ_{ex} = 295 nm) with a blue shift which indicates that LSE interacted with BSA by altering the Trp microenvironments. The dynamic or static type of mechanism usually induces the quenching process and these two are differed by temperature on quenching rate constants where it expected to decrease with raised temperature for static and vice versa for dynamic. Static quenching involves the complex formation at ground state whereas dynamic concern to molecular diffusion at excited state. Stern–Volmer equation (1) analysis the quenching mechanism on fluorescence data [10]:

$$F_0/F = 1 + k_q\tau_0[Q] = 1 + K_{SV}[Q] \quad (1)$$

$$k_q = K_{SV}/\tau_0 \quad (2)$$

where, F and F_0 are BSA fluorescence intensities with and without LSE, respectively.

k_q (for diffusion of bimolecular in dynamic is 2.0 $\times 10^{10}$L mol^{-1}s^{-1}) and K_{SV} are constants of rate and Stern–Volmer quenching, respectively. $[Q]$andτ_0(~2.7 $\times 10^{-9}$ s) are a concentration of LSE and fluorescence lifetime of biopolymer without LSE, respectively. Stern−Volmer plot from Fig. 6A at 295, 303 and 311 K gives k_q (of order 10^{13}L mol^{-1}s^{-1}) and K_{SV} values (Table 3) which were deceased as temperature rises. Therefore, LSE forms a complex with BSA by static quenching.

Modified Stern–Volmer plot (Fig. 6B) from equation (3) further estimates the static quenching for LSE−BSA system.

$$F_0/(F_0 - F) = (1/f_a) + (1/K_a f_a[Q]) \quad (3)$$

wheref_a and K_a is the accessible fluorescence fraction to LSE and a constant of effective static quenching, respectively (Table 3). Decreased K_a values with raised in temperature promote static quenching and the established f_a values become higher as temperatures increment consequential; at higher temperature large BSA is available for quenching by LSE.

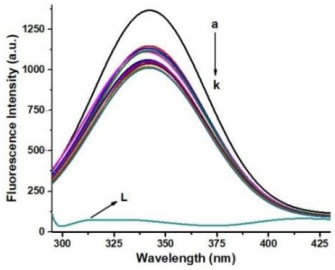

Figure 5. At 303 K, BSA (3.30×10^{-6}mol L^{-1}) fluorescence emission spectrumwith increased LSE (0.0, to 5.50×10^{-6}mol L^{-1}) concentrations and curve L is LSE (3.30×10^{-6}mol L^{-1}) alone.

Table 1. Determined secondary structures by FT−IR and CD at 303 K.

System		Secondary structures (%)				
		β-sheet	Random coil	α-helix	β-turn	β-antiparallel
FT−IR	Free BSA	1.54 ± 0.06	11.25 ± 0.05	54.96 ± 0.02	27.60 ± 0.05	4.65 ± 0.08
	LSE−BSA	0.210 ± 0.09	20.29 ± 0.04	48.06 ± 0.10	20.80 ± 0.08	10.63 ± 0.06
CD	Free BSA	2.34 ± 0.03	10.61 ± 0.02	56.03 ± 0.09	25.78 ± 0.06	5.31 ± 0.04
	LSE−BSA	0.83 ± 0.01	22.94 ± 0.07	46.73 ± 0.05	19.60 ± 0.04	9.97 ± 0.09

Table 2. Characterized FT−IR spectral peaks at 303 K.

System	Amide I (cm^{-1})					Amide II (cm^{-1})
	1615-1637	1638-1648	1649-1660	1660-1680	1680-1692	1548
Free BSA	1625 ± 0.54	1637 ± 0.81	1657 ± 0.85	1672 ± 0.12	1686 ± 0.45	1542 ± 0.96
LSE−BSA	1622 ± 0.19	1640 ± 0.53	1651 ± 0.44	1679 ± 0.59	1683 ± 0.16	1545 ± 0.47

3.5. Binding parameters to LSE − BSA system. In the assumption that BSA has independent binding sites for LSE−BSA quenching process, the binding constant (K_b) and binding sites in number (n) are determined from the following equation [11];

$$\log[(F_0 - F)/F] = \log K_b + n\log[Q] \quad (4)$$

Accordingly, LSE binding into BSA with their K_b and n values were calculated from the plot as shown in Fig. 6C and are illustrated in Table 4 revealsthat n values are about 1 indicating only one LSE binding to BSA. Furthermore, the values of K_b were in the order 10^5 exhibited strong binding interactions between LSE and BSA. Meanwhile, K_b values decreasing trend suggesting that, LSE−BSA complex stability is decreased at increased temperature and thus confirmed static quenching.

Table 3. Different quenching constants at for LSE−BSA system.

T (K)	K_{SV} (L mol^{-1})× 10^5	k_q (L mol^{-1}s^{-1}) × 10^{13}	K_a (L mol^{-1}) × 10^5	f_a
295	2.39 ± 0.08	8.85± 0.01	3.09 ± 0.05	0.17
303	1.89± 0.04	7.00 ± 0.07	2.31 ± 0.06	0.26
311	1.61 ± 0.05	5.96 ± 0.06	0.97 ±0.09	0.68

K_{SV} is Stern−Volmer quenching constant, k_q is quenching rate constant and K_a is effective static quenching constant

Table 4. At different temperatures, binding and thermodynamic attributes to LSE−BSA system.

T (K)	K_b (L mol^{-1}) × 10^5	n	ΔG (k J mol^{-1})	ΔH (k J mol^{-1})	ΔS (J mol^{-1}K^{-1})
295	22.80 ± 0.06	1.426	−35.99	−211.43	−594.7
303	3.52 ± 0.01	1.236	−31.24		
311	0.39 ±0.05	1.012	−26.48		

K_b is binding constant, n is number of binding sites, ΔG is change is Gibb's free energy, ΔH is change in enthalpy and ΔS is change in entropy

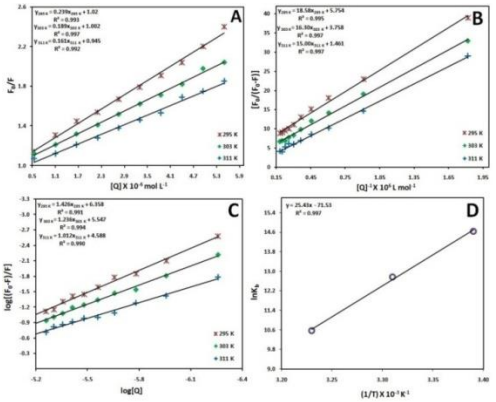

Figure 6. (A) Stern−Volmer (B) Modified Stern−Volmer (C) analyzed binding parameters and (D) van't Hoff plot at 295, 303 and 311 K.

3.6. Thermodynamics to characteristic binding forces. Numerous weaken non-covalent interactions: Vander Waals, hydrophobic, electrostatic etc are composed the binding force within biological macromolecules and small molecules bounded form [12]. To explore the LSE − BSA interaction forces, thermodynamic parameters were evaluated from equation (5) and van't Hoff equation (6):

$$\Delta G = \Delta H - T\Delta S \quad (5)$$

$$\ln K_b = (-\Delta H/RT) + (\Delta S/R) \quad (6)$$

where, ΔH, ΔS, T and R are referred to change in enthalpy, change in entropy, temperature and gas constant, respectively. From equation (5), ΔG (change in free energy) was obtained at 295, 303 and 311 K after calculation of ΔH and ΔS values using equation (6) from the plot of $\ln K_b$ adverse to $1/T$ which is elucidated in Fig. 6D (Table 4).

The accomplished negative ΔH and ΔG values have manifested that exothermic and spontaneous process of LSE − BSA interaction. Based on Ross and Subramanian perspective [13], negative ΔH and ΔS values indicate binding forces for LSE−BSA system was Vander Waals with hydrogen bonding. Also, ΔG was explicitly entropy driven due to the low value ofΔH compare to ΔS.

3.7. Resonance energy transfer by fluorescence. Distance (r) between LSE and BSA (Trp-134/Trp-213) could be analyzed from Förster theory [14]. $E$is efficiency, calculated as;

$$E = R_0^6/(R_0^6 + r^6) = (F_0 - F)/F_0 \quad (7)$$

where, R_0 is a critical distance at 50% of E determined as;

$$R_0^6 = 8.8 \times 10^{-25} K^2 N^{-4} \Phi J \quad (8)$$

where, K^2 (2/3) is a factor associated to the geometry of LSE and BSA dipoles, N (1.336) is medium refractive index, Φ (0.118) is BSA quantum yield without LSE at fluorescence and J is overlap integral from Fig. 7, which is evaluated as;

$$J = \{\sum[F_d(\lambda)\varepsilon_a(\lambda)\lambda^4\Delta\lambda]\}/\{\sum[F_d(\lambda)\Delta\lambda]\} \quad (9)$$

where $F_d(\lambda)$ is BSA fluorescence intensity, $\varepsilon_a(\lambda)$ is LSE molar extinction coefficient at wavelength λ and obtained E, r, R_0 and J are 26.31%, 0.19 Å, 0.16 Å and 8.90×10^{-16}cm^{3}L mol^{-1}, respectively. Since r and R_0 lies less than 0.8 Å revealing energy transfer from BSA (Trp-134/Trp-213) to LSE was achieved with high probability. Moreover, r>R_0 indicating the presence of static quenching due to LSE−BSA complex formation.

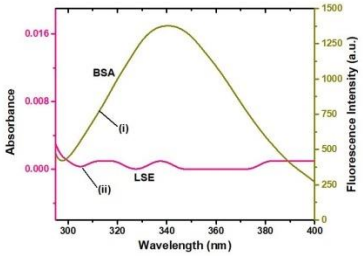

Figure 7. Overlapped spectrum for BSA and LSE at 303 K and both were of 3.30×10^{-6}mol L^{-1} concentrations.

3.8. Synchronous fluorescence. Fig. 8 presents synchronous fluorescence spectra of LSE − BSA system, which shows decreased intensity as raise in LSE concentrations for Tyr and Trp.Polarity and microenvironmentalchanges around chromophoric (Tyr/Trp) residues could be revealed by a spectral shift in synchronous fluorescence [15]. Redshift from Fig. 8B is signifying microenvironmental alteration and more hydrophilic nature for Trp, but no shift was observed for Tyr.

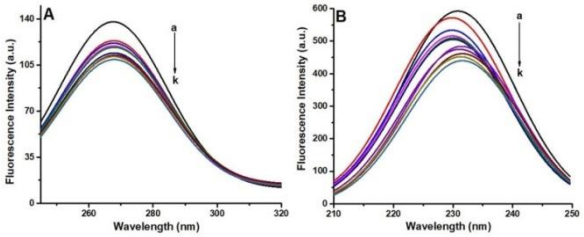

Figure. 8. Synchronous fluorescence spectra at 303 K to (A)Tyr and (B) Trp where BSA was 3.30×10^{-6}mol L^{-1} and LSE was varied as 0.0 to 5.50×10^{-6}mol L^{-1}.

3.9. 3D fluorescence. BSA 3D fluorescence spectra are depicted in Fig. 9 constitutes peaks 'a' ($\lambda_{em} = \lambda_{ex}$, Rayleigh first order), 'b' ($\lambda_{em} = 2\lambda_{ex}$, Rayleigh second order), '1' (for Tyr/Trp, $n \rightarrow \pi^*$ transition) and '2' (for polypeptide backbone, $\pi \rightarrow \pi^*$ transition) [16] with and without LSE. The decrement in the intensity of these 4 distinct peaks (Table 5) has suggested that the conformational and microenvironment (Tyr/Trp) alteration in BSA under the LSE influence by forming LSE −BSA complex.

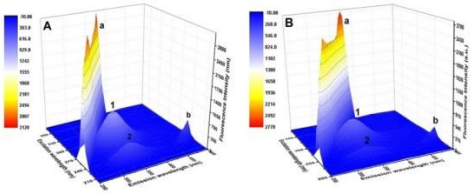

Figure 9. 3D spectra for fluorescence at 303 K: (A) free BSA (3.30×10^{-6}mol L^{-1}) and (B) LSE−BSA system where LSE maintained at 198×10^{-6}mol L^{-1} concentration.

Table 5. 3D fluorescence exemplify at 303 K.

Peak position ($\lambda_{ex}/\lambda_{em}$nm/nm)	Peak	Intensity	
270/270→ 370/370		Free BSA	LSE−BSA
250/500	a	2413 → 3120	1711 → 2761
280/340	b	454.1	248.3
230/340	1	971.4	607.4

3.10. Site-specifically LSE binding to BSA. In order tosubstantiate binding site of LSE on BSA, displacement experiments were executed using site markers, warfarin to site I, ibuprofen exclusively binds to II and digitoxin to III [17]. The k_b values displayed in Table 6, calculated from plot Fig. 10A for LSE−BSA system with site markers. These manifestations have suggested that a significant decrease in k_b value acquire for ibuprofen presence and nearly no deviation was observed for $k_b$value on LSE−BSA system with warfarin and digitoxin. Hence, ibuprofen competes with LSE on BSA binding at site II. Therefore, LSE binds BSA at sub-domain IIIA.

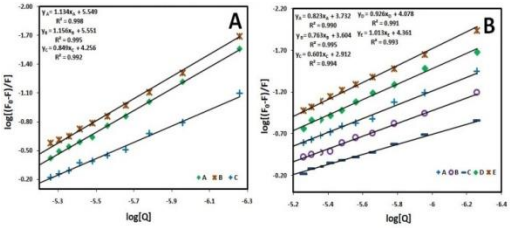

Figure 10. Determined binding constants at 303 K: (A) warfarin-A, digitoxin-B and ibuprofen-C and (B) Fe^{2+}-A, Zn^{2+}-B, Co^{2+}-C, Ca^{2+}-D and Na^{+}-D ions for LSE−BSA system.

Table 6. Binding constant of LSE−BSA system at 303 K with various situations.

system	K_b (L mol^{-1})
BSA−LSE	$3.52 \pm 0.08 \times 10^5$
BSA−LSE−warfarin	$3.54 \pm 0.02 \times 10^5$
BSA−LSE−ibuprofen	$1.80 \pm 0.01 \times 10^4$
BSA−LSE−digitoxin	$3.56 \pm 0.09 \times 10^5$
BSA−LSE−Zn^{2+}	$4.02 \pm 0.06 \times 10^3$
BSA−LSE−Na^{+}	$2.29 \pm 0.07 \times 10^4$
BSA−LSE−Fe^{2+}	$5.39 \pm 0.10 \times 10^3$
BSA−LSE−Ca^{2+}	$1.19 \pm 0.04 \times 10^4$
BSA−LSE−Co^{2+}	$8.16 \pm 0.6 \times 10^2$

$K_b$is binding constant

3.11. Metal ions on LSE−BSA system. Metal ions can contribute an ultimate role in various protein-based coordinate bonds in the human body. Therefore in plasma, the interaction of LSE with BSA can be affected by metal ions. The examined effect of inorganic cations (Zn^{2+}, Na^{+}, Fe^{2+}, Ca^{2+} and Co^{2+}) on k_b value of LSE−BSA system using equation (4) is classified in Table 6 (Fig. 10B). LSE and metal ions, for BSA were not situated in the identical domain, and beyond no direct competitiveness between metal ions and LSE, so that formed metal ion−BSA complexes decreased k_b value for studied metal ions. Thus, this affects the alteration in BSA conformation, which may affect LSE binding kinetics.

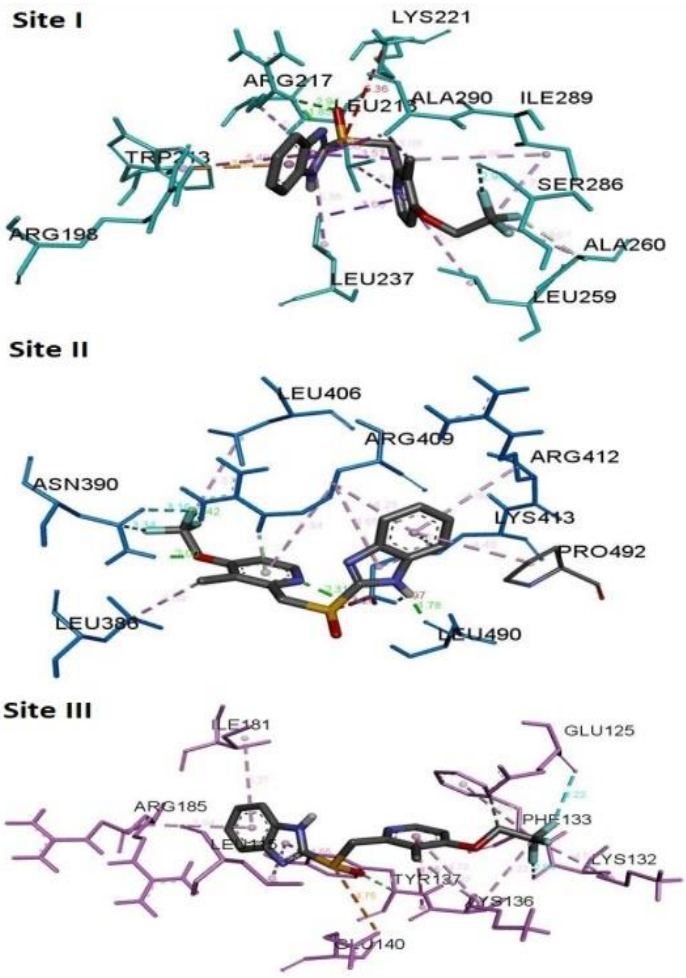

Figure 11. Molecular docking depictions to LSE−BSA system at diverse sites.

Table 7. Favorable binding characteristics of LSE to BSA at site II from molecular docking examinations.

Binding site	Interactions		Amino acid – LSE atom
	Type	Distance (Å)	
	Vander Waals	–	PHE402
		–	LEU452
		–	LEU429
		–	TYR410
		–	SER488
		–	THR491
	Conventional Hydrogen Bond	2.00	ASN390: HD22 – O1
		2.42	ARG409: HH21 – F2
Site II (IIIA)		2.31	LYS413: HZ1 – N3
		1.78	LEU490: O – H3
	Halogen (Fluorine)	3.16	ASN390: OD1 – F2
		3.34	ASN390: CG – F1
	Unfavorable Positive-Positive	3.26	LYS413: NZ – S1
	Unfavorable Donor-Donor	1.97	LYS413: HZ2 – H3
	Pi-Donor Hydrogen Bond	2.27	ARG409: HE – aromatic ring 3
	Pi-Alkyl	5.34	ARG409: (CB-CG-CD1) – aromatic ring 3
		4.65	ARG409: (CB-CG-CD1) – aromatic ring 2
		4.23	ARG409: (CB-CG-CD1) – aromatic ring 1
		4.55	LYS413: (CB-CG-CD1) – aromatic ring 2
		4.46	LYS413: (CB-CG-CD1) – aromatic ring 1
		4.89	ARG412: (CB-CG-CD1) – aromatic ring 1

Binding site	Interactions		Amino acid – LSE atom
		4.48	PRO492: aromatic ring 1 – (CB-CG-CD)
	Alkyl	3.38	LEU406: (CD1-CG-CD1) – C16
		4.47	LEU386: (CD1-CG-CB) – C8

3.12. Molecular docking analysis. Molecular docking was conducted to predict LSE binding site on BSA and to confirm displacement experimental results are described above. LSE binding mode by cluster analysis at 3 binding sites wasperformed independently and best conformations are represented as in Fig. 11 and Table 7. More negative energy and cluster mode retrieved for site II are -33.26 KJ mol^{-1} and 85, respectively in comparison to the other two sites.

Table 8. LSE−BSA system containing distinct energies as applied Lamarckian Genetic Algorithm.

Rank	Run	ΔG (KJ mol^{-1})	$E_{inter-mol}$ (KJ mol^{-1})	$E_{vdw+HB+desol}$ (KJ mol^{-1})	E_{Elec} (KJ mol^{-1})
1	75	−33.26	−40.76	−39.16	−1.58
2	39	−33.22	−40.75	−39.70	−1.00
3	26	−33.09	−40.58	−39.70	−0.92
4	86	−32.46	−39.95	−39.24	−0.71
5	18	−28.70	−36.19	−35.94	−0.25

ΔG is the binding free energy,

$E_{inter-mol}$ is the intermolecular interaction energy; sum of Vander Waals energy, hydrogen bonding energy, desolvation free energy and electrostatic energy,

$E_{vdw+HB+desol}$ is the sum of Vander Waals energy, hydrogen bonding energy and desolvation free energy

E_{Elec} is the electrostatic energy

Therefore, a desirable binding site for LSE was site II and this is good congruence with displacement experiments. The appropriate predicted site II for LSE on BSA was further analyzed to find out binding modes. From Table 7, LSE at site II proximity is covered several ionic and polar residues. The data in Table 8 shows less value of $E_{vdw+HB+desol}$ as compared to E_{Elec}. Thereby, these observations affiliate LSE exclusively involves Vander Waals and hydrogen bond with BSA at site II i.e. sub-domain IIIA.

4. CONCLUSIONS

At pH 7.40, LSE to BSA binding interaction was executed from molecular docking various spectroscopic disciplines. Results show that LSE statically quenched BSA by binding efficiently thereby evaluated the assorted binding parameters. Examinations from molecular docking and competitive site markers provide sub-domain IIIA as a binding site for LSE of BSA. Determined thermodynamics depicts the van der Waals and hydrogen bonds as substantial binding forces to LSE−BSA interaction. FT−IR and CD inspected BSA secondary structure alterations upon LSE binding. Between BSA and LSE energy was transferred as noticed from FRET. UV-vis, 3D and synchronous fluorescence successfully gave detailed study over LSE interaction on microenvironment amendments in BSA. Strong BSA to LSE binding was diminished when Zn^{2+}, Na^{+}, Fe^{2+}, Ca^{2+} and Co^{2+} ions have interfered.

5. REFERENCES

1. Atmanand, M.B.; Arunkumar, T.B.; Naveen, M.G.; Sharanappa, T.N.Characterization of the binding and conformational changes of bovine serum albumin upon interaction with antihypertensive olmesartanmedoxomil. *Journal of Molecular Structure* **2019**, *1179*, 269-277, https://doi.org/10.1016/j.molstruc.2018.10.089.
2. Magdalena, M.; Agnieszka, L.Study of the binding interactions between uric acid and bovine serum albumin using multiple spectroscopic techniques. *Journal of Molecular Liquids* **2019**, *276*, 595-606, https://doi.org/10.1016/j.molliq.2018.12.026.
3. Lansoprazole. MedicineNet. https://www.medicinenet.com/lansoprazole/article.htm (accessed 4 March **2019**).
4. Lansoprazole. Healthline. https://www.healthline.com/health/lansoprazole-oral-capsule-sprinkles (accessed 4 March **2019**).
5. Lansoprazole. RxList. https://www.rxlist.com/consumer_lansoprazole_prevacid/drugs-condition.htm. (accessed 4 March **2019**).
6. Mohd, S.A.; Hamad, A.A.Experimental and computational investigation on the molecular interactions of safranal with bovine serum albumin: Binding and anti-amyloidogenic efficacy of ligand. *Journal of Molecular liquids*, **2019**, *278*, 385-393, https://doi.org/10.1016/j.molliq.2019.01.034.
7. Glazer, A.N.; Smith, E.L. Studies on the ultraviolet difference spectra of proteins and polypeptides. *Journal of Biological Chemistry* **1961**, *236*, 2942-2947.
8. Yang, P.; Gao, F. *The Principle of Bioinorganic Chemistry*, 1st ed.; Science Press: Beijing, China, 2002; pp. 349-492.
9. Shi, J.H.; Zhou, K.L.; Lou, Y.Y.; Pan, D.Q. Multi-spectroscopic and molecular modeling approaches to elucidate the binding interaction between bovine serum albumin and darunavir, a HIV protease inhibitor. *Spectrochimica Acta Part A: Molecular and Biomolecular Spectroscopy* **2018**, *188*, 362-371,https://doi.org/10.1016/j.saa.2017.07.040.
10. Chen, G.Z.; Huang, X.Z.; Xu, J.G.; Zheng, Z.Z.; Wang, Z.B. *The Methods of Fluorescence Analysis*, 2nd ed.; Science Press: Beijing, China 1990.
11. Lakowicz, J.R. *Principles of fluorescence spectroscopy*, 3rd ed.; Springer Science & Business Media. Berlin, Germany, 2007.
12. Reshma; Sandeep, K.V.; Indrapal, K.; Manmohan, L.S.; Kallol, K.G.Spectroscopic studies on in vitro molecular interaction of highly fluorescent carbon dots with different serum albumins. *Journal of Molecular Liquids* **2018**, *255*, 279-287, https://doi.org/10.1016/j.molliq.2018.01.146.
13. Ross, P.D. Subramanian, S. Thermodynamics of protein association reactions forces contributing to stability. *Biochemistry* **1981**, *20*, 3096-3102, https://doi.org/10.1021/bi00514a017.
14. Shi, J.H.; Lou, Y.Y.; Zhou, K.L.; Pan, D.Q. Elucidation of intermolecular interaction of bovine serum albumin with Fenhexamid: A biophysical prospect. *Journal of Photochemistry & Photobiology, B: Biology* **2018**, *180*, 125-133, https://doi.org/10.1016/j.jphotobiol.2018.01.025.

15. Congbin, Y.; Peiwen, D.; JinPing, F.; Hui. X.; Qiufang, J.; Guobin R.; Yun, T.;Wenyun, Z.; Guixia, L.; Fuzheng, R. Improving the physicochemical properties of bicalutamide by complex formation with bovine serum albumin. *European Journal of Pharmaceutical Sciences* **2017**, *106*, 381-392, https://doi.org/10.1016/j.ejps.2017.05.059.
16. Yusra, R.;Shumaila, A.; Mohammad, T.Interaction of pirenzepine with bovine serum albumin and effect of β-cyclodextrin on binding: A biophysical and molecular docking approach. *Archives of Biochemistry and Biophysics* **2018**, *652*, 27-37, https://doi.org/10.1016/j.abb.2018.06.005.
17. Samima, K.; Riyazuddeen,Gulam, R.A comparative biophysical and in-silico studies on the interactions of ticlopidine hydrochloride with two serum albumins. *Journal of Chemical Thermodynamics* **2019**, *131*, 9-20, https://doi.org/10.1016/j.jct.2018.10.017.

6. ACKNOWLEDGEMENTS

Manjushree Makegowda (author) gratefully acknowledges the UGC−BSR, New Delhi, India, for awarding research fellowship. Yet authors thank IOE, Mysuru, India for spectral assessments and CATERS-CSIR-CLRI, Chennai, India for CD measurements.